Available online at www.sciencedirect.com
ScienceDirect
International Journal of Mass Spectrometry 267 (2007) 284–287
www.elsevier.com/locate/ijms

Thermochemical stabilities of the gas-phase cluster ions of halide ions with rare gas atoms

Akira Wada, Akira Kikkawa, Teruaki Sugiyama, Kenzo Hiraoka*

Clean Energy Research Center, University of Yamanashi, Takeda-4, Kofu 400-8511, Japan

Received 8 November 2006; received in revised form 26 February 2007; accepted 27 February 2007
Available online 4 March 2007

Abstract

Gas-phase clustering reactions of halide ions (X^-) with rare gas atoms (Rg) have been investigated using a pulsed-electron beam high-pressure mass spectrometer. The thermochemical stability of the cluster ions $X^-(Rg)_n$ has been determined. To evaluate bond energies that are difficult to obtain experimentally, ab initio calculations were also carried out. Among the cluster ions investigated, the interaction between the hardest F^- ion and the softest Xe atom was found to be strongest (6.3 kcal/mol).

© 2007 Elsevier B.V. All rights reserved.

Keywords: High-pressure mass spectrometry; Cluster ion; Rare gas; Halide ion

1. Introduction

Micro-clusters are the incipient stage of matter and their natures and reactivities provide basic information in the fields of gaseous ion chemistry, nuclear physics, radiation chemistry, quantum electronics, phase transitions, crystal growth, surface science, catalysis, solution chemistry, biochemistry, etc. The thermochemical stabilities and reactivities of gas-phase cluster ions are particularly helpful in understanding the mechanisms of the complicated phenomena occurring in the multibody system.

The interaction between the halide ions X^- and rare gas atoms gives the most fundamental aspect for the ion–molecule interaction because both halide ions and rare gas atoms have closed shells. The bond energies of $X^-(Rg)_n$ clusters were measured by the swarm method [1–3] and summarized by Gatland [4]. Neumark and coworkers investigated $Br^-(Ar)_n$, $I^-(Ar)_n$, $I^-(Xe)_n$ and $Cl^-(Ar)_1$ clusters by anion zero electron kinetic energy (ZEKE) and partially discriminated threshold photodetachment spectroscopy [5–7]. The experiment yielded size-dependent electron affinities and electronic state splittings of the halogen atoms in the neutral clusters formed by photodetachment. Archibond et al., using ab initio calculations, obtained potential energy curves for the interaction of a fluoride anion with a He atom and a Ne atom by supermolecular calculations [8]. The bond dissociation energies for $F^- \cdots He$ and $F^- \cdots Ne$ were predicted to be 0.15 and 0.29 kcal/mol, respectively. Zeiri studied the structure and dynamics of Cl and Br ions and atoms in Xe clusters by a genetic algorithm based search method [9]. The calculations indicated that for large clusters both Cl and Cl^- were located inside the Xe cluster, while Br and Br^- adsorb onto the cluster surface. Bowen and coworkers measured negative ion photoelectron spectra of the solvated anion clusters $O^-(Ar)_n$ ($n = 1$–26, 34). They found that the first solvation shell closes at $n = 12$. Furthermore, magic numbers in the energetic data and in the mass spectrum suggest that $O^-(Ar)_n$ clusters of sizes $n = 12$–34 are structurally very similar to homogeneous rare gas clusters [10].

In the present work, the systematic study on the thermochemical stabilities of the cluster ions $X^-(Rg)_n$ was made by a high-pressure mass spectrometry. It was found that the $F^- \cdots Xe$ is most strongly bound and there is a small gap in the binding energies for $F^-(Xe)_n$ between $n = 1$ and 2. This suggests a small charge dispersal in the complex $[F \cdots Xe]^-$.

2. Experimental

The experiments were made with a pulsed electron beam high-pressure mass spectrometer [11,12]. Equilibrium measurements for the clustering reaction (1) were made by introducing X^--forming reagent gases (NF_3 for F^-, CCl_4 for Cl^-, CH_2Br_2

---

* Corresponding author.
E-mail address: hiraoka@yamanashi.ac.jp (K. Hiraoka).

1387-3806/$ – see front matter © 2007 Elsevier B.V. All rights reserved.
doi:10.1016/j.ijms.2007.02.053

Table 1
Thermochemical data, $-\Delta H^{\circ}_{n-1,n}$ (kcal/mol) and $-\Delta S^{\circ}_{n-1,n}$ (cal/mol K) for clustering reactions, $X^-(Rg)_{n-1,n} + Rg = X^-(Rg)_n$, for X = F, Cl, Br, and I, and Rg = He, Ne, Ar, Kr and Xe

	1		2		3	
	$-\Delta H^{\circ}_{n-1,n}$	$-\Delta S^{\circ}_{n-1,n}$	$-\Delta H^{\circ}_{n-1,n}$	$-\Delta S^{\circ}_{n-1,n}$	$-\Delta H^{\circ}_{n-1,n}$	$-\Delta S^{\circ}_{n-1,n}$
$F^-(He)_{n-1,n} + He = F^-(He)_n$	0.15[a]					
$F^-(Ne)_{n-1,n} + Ne = F^-(Ne)_n$	0.29[a]					
$F^-(Ar)_{n-1,n} + Ar = F^-(Ar)_n$	~2.0	(20)[b]				
$F^-(Kr)_{n-1,n} + Kr = F^-(Kr)_n$	4.1 ± 0.3	19 ± 3				
$F^-(Xe)_{n-1,n} + Xe = F^-(Xe)_n$	6.3 ± 0.3 6.5[c]	16 ± 3	5.2 ± 0.3	17 ± 0.3	5.0 ± 0.4	19 ± 4
$Cl^-(Ar)_{n-1,n} + Ar = Cl^-(Ar)_n$	1.5[d]					
$Cl^-(Kr)_{n-1,n} + Kr = Cl^-(Kr)_n$	2.8 ± 0.4	19 ± 4				
$Cl^-(Xe)_{n-1,n} + Xe = Cl^-(Xe)_n$	4.2 ± 0.3 3.1[e]	19 ± 3	3.7 ± 0.4	20 ± 4		
$Br^-(Ar)_{n-1,n} + Ar = Br^-(Ar)_n$	1.36[f]					
$Br^-(Kr)_{n-1,n} + Kr = Br^-(Kr)_n$	<2.7 2.01[f]					
$Br^-(Xe)_{n-1,n} + Xe = Br^-(Xe)_n$	3.6 ± 0.3	16 ± 3				
$Br^-(Xe)_{n-1,n} + Xe = Br^-(Xe)_n$	3.35[f]					
$I^-(Xe)_{n-1,n} + Xe = I^-(Xe)_n$	~2.8	(16)[b]				

[a] Ref. [8].
[b] Entropy value arbitrarily assumed.
[c] Ref. [3].
[d] Ref. [7].
[e] Ref. [4]
[f] Ref. [2].

for Br^-, and CH_3I for I^-) into the ~3 Torr reagent rare gas (Rg) through a stainless steel capillary.

$$X^-(Rg)_{n-1} + Rg = X^-(Rg)_n \quad (1)$$

The measurements were made down to the low temperature limit at which the X^--forming reagent gases started to condense on the wall of the ion source. With the condensation of X^--forming reagent gases on the ion source, the ion signals of X^- disappeared completely.

3. Results and discussion

The results for the experimentally determined thermochemical data are summarized in Table 1 together with those obtained by other investigators. Due to the relatively high temperature limits due to the condensation of X^--forming reagent gases, the cluster ions $X^-(He)_n$, $X^-(Ne)_n$, $Br^-(Ar)_n$, $Br^-(Kr)_n$, $I^-(Ar)_n$, and $I^-(Kr)_n$ could not be observed under the present experimental conditions. The bond energy for $Br^-(Kr)_1$ could only be predicted to be smaller than 2.7 kcal/mol.

The temperature dependence of the equilibrium constants for the clustering reaction $F^-(Xe)_{n-1} + Xe = F^-(Xe)_n$ (n = 1–3) is shown as van't Hoff plots in Fig. 1. In the figure, there appears a gap between $n = 1$ and 2 and the plots with $n = 2$ and 3 are much closer to each other. This suggests some charge dispersal in the complex, i.e., [$F^- \rightarrow Xe$]. This finding is reminiscent of the fact that Xe bonds with electronegative elements (e.g., F, O, and Cl) which contracts its d-orbital. The charge transfer from F^- to the vacant 4f orbital of the Xe atom may also take place to some extent in the moiety $F^-\cdot Xe$.

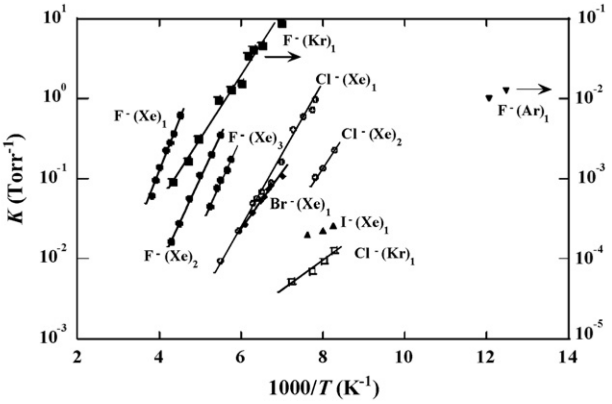

Fig. 1. van't Hoff plots for the clustering reaction $X^-(Rg)_{n-1} + Rg = X^-(Rg)_n$ for X = F, Cl, Br, and I and Rg = Ar, Kr, and Xe.

In Fig. 2, the bond energies for $X^-(Rg)_1$ measured in this work are summarized. As expected, the bond energies of $X^-(Rg)_1$ for respective X^- are in the order of the polarizabilities of the rare gas atoms (Xe: 4.02 Å^3, Kr: 2.48 Å^3, Ar: 1.64 Å^3, Ne: 0.408 Å^3, and He: 0.206 Å^3 [13]). The bond energies of $F^-(Rg)_1$ and $Cl^-(Rg)_1$ are found to decrease quite rapidly with decrease of the size of the Rg atoms. This clearly indicates that the ion-induced dipole interaction plays a major role in the cluster ions $X^-(Rg)_1$.

The ab initio calculations at the CCSD(T)/aug-cc-pVTZ level of theory level were carried out on the $X^-(Rg)_1$ system for X = F, Cl, Br, and I, and Rg = He, Ne, Ar, Kr, and Xe. We have also performed geometry optimization calculations for $X^-(Xe)_2$ and $X^-(Xe)_3$, X = F, Cl using B3LYP and then single point calculations at B3LYP for optimized structures by

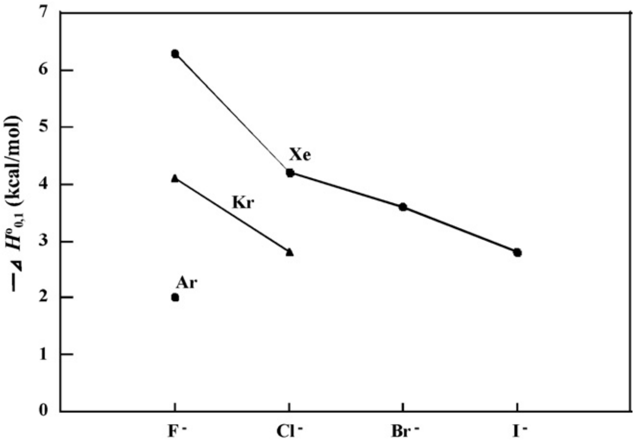

Fig. 2. Bond energies ($-\Delta H^{\circ}_{0,1}$) for the cluster ions $X^{-}(Rg)_1$ for X = F, Cl, Br, and I and Rg = Ar, Kr, and Xe.

Table 2

Ab initio calculated binding energy $-\Delta H^{\circ}$ (kcal/mol), bond length (Å), and harmonic frequency (cm^{-1}) for $X^{-}(Rg)_1$ using CCSD(T)/aug-cc-pVTZ level of theory

	F	Cl	Br	I
He				
Bond energy	0.20	0.11	0.09	0.11
Bond energy (with BSSE)	0.17	0.10	0.08	–
Bond length	3.26	4.05	4.17	4.51
Harmonic frequency	46.19	30.43	30.16	26.30
Ne				
Bond energy	0.47	0.29	0.25	0.27
Bond energy (with BSSE)	0.38	0.23	0.19	–
Bond length	3.18	3.83	3.99	4.25
Harmonic frequency	46.43	28.41	24.92	21.79
Ar				
Bond energy	2.39	1.36	1.17	1.10
Bond energy (with BSSE)	2.20	1.23	1.02	–
Bond length	3.04	3.72	3.86	4.16
Harmonic frequency	92.40	52.39	55.63	33.95
Kr				
Bond energy	3.67	2.02	1.73	1.74
Bond energy (with BSSE)	3.41	1.84	1.55	–
Bond length	3.01	3.72	3.92	4.17
Harmonic frequency	101.00	55.10	39.70	32.32
Xe				
Bond energy	6.43	3.02	5.53	2.64
Bond energy (with BSSE)	–	–	–	–
Bond length	2.96	3.72	3.92	4.20
Harmonic frequency	126.35	63.78	44.30	33.99

using CCSD(T)/aug-cc-pVTZ level of theory. The aug-prefix means that diffuse functions have been supplemented to the plain sets. The small-core relativistic PP correlation consistent basis sets, cc-pVTZ-PP of Peterson et al. [14] were used for Xe and I atoms. Basis set superposition error (BSSE) corrections following the counterpoise method of Boys and Bernardi [15] were applied for all basis sets except molecules including Xe or I atoms. The calculated molecular structures and bond energies of $X^{-}(Rg)_1$ are shown in Table 2. Harmonic vibrational energies are also calculated and used for binding energy calculation. The calculated binding energies for $X^{-}(Rg)$ are in good agreement with experimental values. It is confirmed by the calculations that the binding energy increases with the size of rare gas atom. This is explained by the increase of polarizability with the size of rare gas atom as mentioned before. In a given rare gas, the interaction decreases as the size of halogen atom increases, owing to the dispersion of negative charge in X^{-}.

The optimized structures for $F^{-}(Xe)_2$ and $Cl^{-}(Xe)_2$ at B3LYP/aug-cc-pVTZpp level of theory were determined to be C_{2v} and $D_{\infty h}$, respectively. The binding energies are obtained by CCSD(T) level of calculations at B3LYP/aug-cc-pVTZpp optimized structures. The structure and binding energy of $F^{-}(Xe)_3$ and $Cl^{-}(Xe)_3$ were also obtained and shown in Table 3. Both species have C_{3v} symmetry, with $F^{-}(Xe)_3$ more planar structure than $Cl^{-}(Xe)_3$.

4. Conclusion

Thermochemical stabilities for the cluster ions of halide ions (X^{-}) with rare gas atoms (Rg) were investigated. The bond energy of $F^{-}(Xe)$ is measured to be 6.3 ± 0.3 kcal/mol and some charge transfer from F^{-} to Xe is suggested. The bond energies of $F^{-}(Rg)_1$ and $X^{-}(Xe)_1$ are found to decrease rapidly with Rg = Xe → Kr → Ar and X = F → Cl → Br → I, respectively. This is due to the fact that the interactions between X^{-} and Rg atoms are mainly ion-induced dipole interaction except for $F^{-}(Xe)$.

Theoretically calculated binding energies are in good agreement with the experimental values. While the structure of $Cl^{-}(Xe)_2$ is predicted to be of the structure of $D_{\infty h}$, C_{2v} for $F^{-}(Xe)_2$ and C_{3v} for $F^{-}(Xe)_3$ and $Cl^{-}(Xe)_3$ are theoretically predicted. The less symmetric structures for the latter cases are due to the intra-cluster interaction between the ligand Xe atoms.

Table 3

Calculated binding energy, and structural parameters of $F^{-}(Xe)_2$, $Cl^{-}(Xe)_2$, $F^{-}(Xe)_3$, and $Cl^{-}(Xe)_3$ by CCSD(T)/aug-cc-pVTZpp//B3LYP/ aug-cc-pVTZpp

Cluster ion	Symmetry	r (Å)	D (°)	$-\Delta H^{\circ}$ ($X^{-}(Xe) + Xe \rightarrow X^{-}(Xe)_2$) (kcal/mol)
$F^{-}(Xe)_2$	C_{2v}	2.959	72.8	5.91
$Cl^{-}(Xe)_2$	$D_{\infty h}$	3.911		4.83
Cluster ion	Symmetry	r (Å)	D (°)[a]	$-\Delta H^{\circ}$ ($X^{-}(Xe)_2 + Xe \rightarrow X^{-}(Xe)_3$) (kcal/mol)
$F^{-}(Xe)_3$	C_{3v}	3.11	97.0	5.49
$Cl^{-}(Xe)_3$	C_{3v}	3.94	113.0	5.89

[a] Angle between two $X^{-}Xe$ bonds, where one Xe is on the symmetry axis and the other is off-axis.

References

[1] R.G. Keesee, A.W. Castleman Jr., J. Chem. Phys. Ref. Data. 15 (1986) 1011.
[2] C. DeVreugd, R.W. Wijnaendts van Resandt, J. Los, Chem. Phys. Lett. 65 (1979) 93.
[3] M.G. Thackston, F.L. Eisle, W.M. Pope, H.W. Ellis, E.W. McDaniel, I.R. Gatland, J. Chem. Phys. 73 (1980) 3183.
[4] I.R. Gatland, in: W. Lindinger, T.D. Mark, F. Howarka (Eds.), Swarms of Ions and Electrons in Gases, Springer-Verlag, New York, 1984, p. 44, and references therein.
[5] I. Yourshaw, Y. Zhao, D.M. Neumark, J. Chem. Phys. 105 (1996) 351.
[6] T. Lenzer, M.R. Furlanetto, N.L. Pivonka, D.M. Neumark, J. Chem. Phys. 110 (1999) 6714.
[7] T. Lenzer, I. Yourshaw, M.R. Furlanetto, G. Reiser, D.M. Neumark, J. Chem. Phys. 110 (1999) 9578.
[8] E.F. Archibond, C.-H. Hu, A.J. Thakkar, J. Chem. Phys. 109 (1998) 3072.
[9] Y. Zeiri, J. Phys. Chem. A 102 (1998) 2785.
[10] S.T. Arnold, J.H. Hendricks, K.H. Bowen, J. Chem. Phys. 102 (1995) 39.
[11] P. Kebarle, in: J.M. Farrar, W.S. Saunders Jr. (Eds.), Techniques for the Study of Ion–Molecule Reactions, Wiley, New York, 1971, p. 221.
[12] K. Hiraoka, S. Yamabe, in: K. Kuchitsu (Ed.), Dynamics of Excited Molecules, Elsevier, Amsterdam, 1994, p. 399.
[13] E.W. Rothe, R.B. Bernstain, J. Chem. Phys. 31 (1959) 1619.
[14] K.A. Peterson, D. Figgen, E. Goll, H. Stoll, M. Dolg, J. Chem. Phys. 119 (2003) 11113.
[15] S.B. Boys, F. Bernardi, J. Mol. Phys. 18 (1970) 553.